Biotribology 18 (2019) 100090

Contents lists available at ScienceDirect

Biotribology

journal homepage: www.elsevier.com/locate/biotri

Investigation of CoCrMo material loss in a novel bio-tribometer designed to study direct cell reaction to wear and corrosion products

Radice S., Holcomb T., Pourzal R., Hallab N.J., Laurent M.P., Wimmer M.A.*

Department of Orthopedic Surgery, Rush University Medical Center, Chicago, IL, USA

ARTICLE INFO

Keywords:
Orthopedic implants
CoCrMo alloy
Tribocorrosion
Cell culture medium
Response surface

ABSTRACT

Wear and corrosion in total hip replacement negatively impact implant service-life and patient well-being. The aim of this study was to generate a statistical response surface of material loss using an apparatus, capable of testing the effect of wear and corrosion products *in situ* on cells, such as macrophages. The test chamber of a ball-on-flat tribometer operating inside a CO_2 incubator was integrated with an electrochemical setup and adapted for cell culture work. A 20-test series, following a 2-level 3-factor design of experiments, was performed with a ceramic head in reciprocating rotational motion against a CoCrMo-alloy disc, under constant load. The lubricant was cell culture medium (RPMI-1640 + 10 vol% bovine serum). Response surfaces were generated, which statistically showed the influence of motion amplitude, load, and potential on the total mass loss and wear scar volume of the metallic discs. Potential had the highest impact on the total mass loss, while motion amplitude and load significantly influenced the wear scar volume. The concentrations of the alloy elements found in the lubricants reflected the bulk-alloy stoichiometry. The total concentration of Co released into the lubricant (2.3–63 ppm by total mass loss, 1.5 to 62 ppm by ICP-MS) corresponded well with the known range to trigger cell response. Tribocorrosion tests in the presence of cells and tissues, such as macrophages, lymphocytes and/or synovium, will be carried out in the future.

1. Introduction

Metals are common implant materials used in orthopaedics [1]. They are favored over other materials because of for their strength and structural rigidity allowing full or partial load bearing. However, next to these positive characteristics, wear and corrosion of these implants have long been recognized as a problem [2]. The release of metal ions and particles causes adverse local tissue reactions in the implant surrounding tissue, which clinically present as granulomas, necrotic tissue, pseudotumors, *etc.* While much progress has been made in the understanding of immune responses, there is still an incomplete picture of the interaction of cells with metal degradation products. This is in part due to the unknown composition of the debris, which is generated in a complex tribocorrosive environment *in vivo*.

Recent increases in adverse local tissue reactions from metal implants [3–6] have sensitized the clinical community for the need of a better understanding in the underlying mechanisms to metal wear debris. Until today, the immune reactivity of cells to corrosion products is assessed with diluted metal salts, and/or manufactured metal particles [7]. However, there is concern that these simplified testing models may not represent reality and testing with 'real-time' debris may change the picture.

Energy introduced into the contact by rubbing may shift corrosion reactions away from thermodynamic equilibrium, causing the release of unexpected species before those decay to more stable reaction products over time. These meta-stable species may react with proteins and cells in the vicinity of the implant. For example, the hexavalent Cr is such a candidate in the case of cobalt-chromium-molybdenum (CoCrMo) alloy, and could trigger serious cell damage before it becomes stable at a lower valence [8]. However, there are also less toxic scenarios possible that might be of interest. As such, Mo-IV has been implicated in stabilizing a complex carbonaceous film onto CoCrMo, which can graphitize within the tribocontact [9–12]. While the carbonaceous film itself seems biocompatible [13], the immune response to the generated graphitic material is unknown. Graphene, which is similar in structure than the observed graphitic material, has been associated with the production of inflammatory cytokines when exposed to macrophages [14].

Following earlier examples in the literature [15,16], in this paper, we present the results from tests on a tribometer with an integrated electrochemical setup and cell culture chamber, which we call a bio-tribometer. In particular: a) we describe the mechanical and

* Corresponding author.
E-mail address: markus_a_wimmer@rush.edu (M.A. Wimmer).

https://doi.org/10.1016/j.biotri.2019.100090
Received 21 November 2018; Received in revised form 19 March 2019; Accepted 23 March 2019
Available online 27 March 2019

electrochemical set-up of the apparatus (which has been described at a conceptual level by Pourzal et al. [16]); b) we generate a statistical response surface of material (particle and ion) release as a function of 'load', 'motion amplitude', and 'electrochemical potential', which will be used to derive testing conditions that are biologically meaningful in terms of metal content. Tribocorrosion tests in the presence of cells, such as macrophages, lymphocytes and osteoclasts, and tissues, such as synovium, will be considered for future study. Successful execution of this task would enable the preclinical testing of *in situ* degradation products, which could prove important in the discovery of meta-stable debris.

2. Materials & methods

2.1. Samples and tribocorrosion test system

Discs of CoCrMo-alloy, 12 mm in diameter and 7 mm in height, were cut from a medical grade bar stock (Aubert & Duval Corporation, Bollingbrook, Illinois, USA). The chemical composition of this alloy is in accordance with the ASTM F1537 and ISO 5832-12 standards and is given by the manufacturer as follows (values in wt%): C: < 0.14; Cr: 28.00; Mo: 6.00; Ni: < 1.00; Co: Base; with the addition of nitrogen. The exact contents of Co, Cr and Mo from previous measurements in our lab [17] were respectively 65.5 wt%, 26.7 wt% and 5.7 wt%. The discs' surfaces were grinded and mirror-polished on a semi-automatic Struers MD Gecko machine, from *SiC* foil # 220 up to 1 µm diamond paste. Final surface roughness values were measured on a Scanning White Light Interferometer (Zygo NewView 6300) and were found to be in the order of magnitude of R_a = 10 nm. A ceramic ball (Al_2O_3), 32 mm in diameter, was used as wear counterface.

For lubricant/electrolyte, the following cell culture medium was used: RPMI-1640 (Gibco, ThermoFisher Scientific) with 10 vol% fetal bovine serum (Sigma-Aldrich, lot nr. 192,382) and addition of antibiotics (100 I.U. penicillin +100 µg/ml streptomycin). The cell culture medium RPMI-1640 is composed of different amino acids, vitamins, inorganic salts, D-Glucose, reduced Glutathione and Phenol Red (the latter for pH monitoring). Phenol Red confers the medium to a red/pinkish color at pH 7.3–8.0, an orange/reddish color at pH 6.7–7.2 and a yellowish color at pH 6.0–6.6.

2.2. Mechanical and electrochemical setup

The mechanical test rig is based on a lever arm for the load application in a ball-on-flat wear configuration (Fig. 1A). The ceramic head can be displaced vertically through a sliding frame and is fixed at the height, corresponding to contact with the metallic surface with lever arm at horizontal position. A reciprocating rotation motion is applied to the ceramic head by an actuator fixed in the sliding frame. The metallic disc is hold at one extremity of the lever arm, which consists of a stainless steel bar free to rotate around a fulcrum. Standard weights are positioned on the other extremity of the bar (lever-arm principle).

The mechanical setup is combined with a three-electrode electrochemical cell configuration, connected to a potentiostat (Interface 1000E, Gamry Instruments). The cell is composed of a cylindrical chamber made of PEEK, with 23 ml volume capacity (Fig. 1B). The working electrode is the CoCrMo disc sample, which fits in the middle of the chamber through an O-ring, and exposes to the electrolyte only the polished surface area of 1.1 cm^2. A hole (∅ 4 mm) at the bottom of the PEEK chamber allows for the electric connection of the disc sample to the potentiostat, by means of a copper cable. The Silver/Silver Chloride (SSC) Skinny Reference Electrode (Gamry Instruments) in saturated KCl solution is obliquely held at approximately 2 mm from the CoCrMo-disc surface. The standard potential of the SSC reference electrode is 0.197 V *vs.* SHE [18]. For the counter-electrode, three ∅ 0.5 mm platinum (Pt) wires (annealed, 99.95% metals basis, Fischer Scientific) are woven together and arranged circumferentially along pegs, distributed on the inside wall of the chamber's lid. The surface ratio between the counter electrode and the working electrode is approximately 8:1. The chamber is filled up with 23 ml of cell culture medium.

2.3. Testing protocol and test output

The tests were performed inside a water jacketed CO_2 incubator (Model 2460, Shel Lab, Oregon, USA). The temperature was set to 37 °C and the CO_2 level to 5.0%. In order to equilibrate the temperature, the cell culture medium was placed inside the incubator half an hour before the test. The bulk electrolytes' pH stayed in the range 7.0–7.5, checked visually (red/pinkish coloration of the fluid) and using pH papers. The pH value was held constant thanks to the buffer effect of the sodium bicarbonate in the cell culture medium RPMI-1640, working in conjunction with the controlled CO_2 environment.

The CoCrMo-discs were cleaned in ultrasonic bath (10 min Tergazyme® soap solution +10 min isopropanol +10 min bidistilled water Elix Millipore 15), and placed inside the test chamber. The test chamber was generously rinsed under tap bidistilled water, dried with N_2 gas flow, and placed on the test rig inside the incubator. The ceramic ball was brought in contact with the metallic disc, and the load was applied. The cell culture medium was poured into the chamber. The reference electrode was rinsed with bi-distilled water, and positioned in the chamber. The electrodes were connected to the cables of the potentiostat, introduced in the incubator through a hole in the lateral wall. Before the start of each test, a cleaning potentiostatic cathodic potential of −0.7 V (*vs.* SSC) was applied for 10 min, and the open circuit potential was allowed to stabilize for 50 min. For each wear test, the motion amplitude and the load were set in the range of 20° to 40°, and 15 N to 37 N respectively. The first 10 min after the start of the wear test were kept at open circuit potential, in order to record the initial potential drop typical for wear tests [19]. The potential (0 V, +0.45 V or +0.9 V *vs.* SSC) was then applied until the end of the wear test, which had a total duration of 12 h corresponding to 86,400 cycles at 2 Hz, and the current was consistently measured. After completion of the test, lubricant samples were saved in 1.5 ml Eppendorf tubes, and frozen after each test for Inductively Coupled Plasma Mass Spectroscopy/Optical Emission Spectroscopy (ICP-MS/OES) analysis, as described later in this section.

The design of experiment (DOE) for this study was constructed using response surface methodology (RSM), in order to minimize the number of experimental conditions for three different input parameters in the tribological behavior. Response surface methodology was developed by Box and collaborators in the 1950s [20]. RSM consists of a group of mathematical and statistical techniques that are based on the fit of empirical models to the experimental data, obtained in relation to experimental design; this term derived from the graphical perspective generated after the fit [21].

Each of the three input parameters 'load', 'motion amplitude', and 'electrochemical potential' was tested at two levels (low, high), according to a 2-level 3-factor design of experiment (DOE), with two replicates (n = 2) and a center point (n = 4), for a total of 20 tests. The center point was the midpoint between the high and low levels of each parameter, was included to detect curvature, *i.e.*, a departure of the response surface from linearity. Testing conditions and parameter values are listed in Table 1. The choice of the parameter values for the low and high levels was based on previous experience and publications of the authors [22], while the values at the center point are in the middle between those. The applied load levels of 15, 26, and 37 [N] represent 40, 53, and 66 [MPa] of contact stress after running-in (1800 cycles) [23]. The motion amplitudes 20°, 30° and 40° at 2 Hz are achieved with a controlled trapezoidal velocity profile; they correspond to sliding speeds of approximately 22 mm/s, 34 mm/s and 45 mm/s, respectively.

Three additional tests outside the DOE were run at the following conditions: (1) 37 N load and 40° motion amplitude, at open circuit

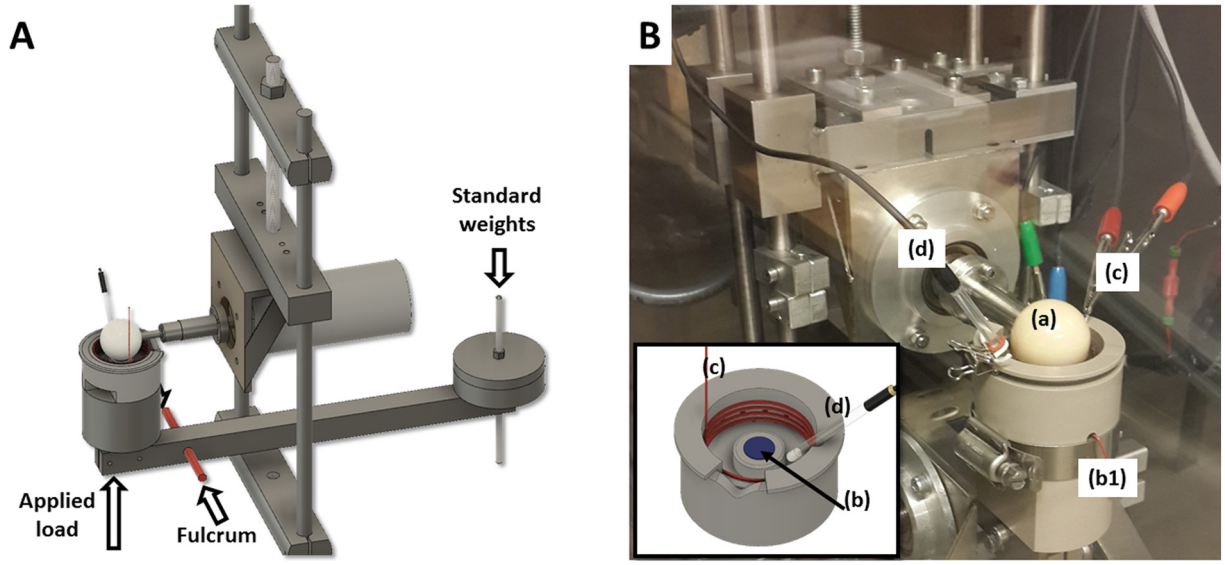

Fig. 1. A) Illustration of the lever-arm principle for the load application. B) Bio-tribometer inside the incubator and simplified drawing of the chamber with the 3-electrodes setup: (a) Al_2O_3 ceramic ball, ∅ 32 mm; (b) CoCrMo metallic disc, ∅ 12 mm (working electrode with cable 'b1'); (c) platinum wire (counter electrode); (d) SSC (Ag/AgCl) reference electrode.

Table 1
The 2-level 3-factor design of experiments of the tribocorrosion tests. The applied load levels of 15 N, 26 N, and 37 N represent respectively 40 MPa, 53 MPa, and 66 MPa of contact stress after running-in.

Wear configuration	Ball-on-flat (Al_2O_3 ball-on-CoCrMo disc)
Medium	Cell culture medium (RMPI-1640 + 10 vol% FBS)
Motion	Reciprocating rotation
Frequency	2 Hz
Time (nr. of cycles)	12 h (86,400 cycles)

Parameters	Amplitude [°]	Load [N]	Potential [V *vs.* SSC]
Level 1 (n = 2)	20	15	± 0.0
Level 2 (n = 2)	40	37	+ 0.9
Center point (n = 4)	30	26	+ 0.45

potential (equivalent to no applied potential); (2) 0.9 V potential and 40° motion amplitude, with no applied load (the ceramic ball was held at reciprocating rotation motion at about 2 mm distance from the CoCrMo-disc); (3) 37 N load and 40° motion amplitude, with 0 V applied potential, for a total duration of 180 h at 2 Hz (1'269'000 cycles).

The primary output measurements for describing the system response were wear scar volume and sample weight loss. The wear scar volume measurement was achieved by White Light Interferometry (Zygo NewView 6300), using a semi-automatic macro available for this application: after an accurate focus of the wear scar surface with the appearance of interference bands, a mask was defined around the wear scar allowing to set the reference plane for the automatic computation of the wear scar volume. Sample weight loss was measured by the difference of sample weight after and before the test using a precision balance (Mettler Toledo AX205 Delta Range, 0.01 mg readout). Secondary output measurements included 'charge density', which was calculated by integration of the current response over the duration of the wear test, and 'metal content in medium'. In order to determine the metal content, the Co, Cr, and Mo concentrations were measured using ICP-MS after sample filtration and HNO_3 acid digestion of the medium in the Anton Paar Multiwave Microwave System: 1 g of the samples were dissolved with a mixture of 2 ml HNO_3 conc and 2 ml H_2O. The digestion was made by use of a microwave system in a 16 ml TFM-Microwave container. The containers have been shut and put into the Microwave applying 800 W of Microwave power temperatures of 200 °C are achieved. A complete decomposition of the entire sample is achieved after 35 min. After cooling to room temperature the containers will be opened under a clean bench with filter, capable to provide class 10 clean air to protect the operator from occasionally appearing NO_x and to protect the samples from contamination. Further, to rule out any degradation of the Al_2O_3 ceramic ball, media samples were analyzed for aluminum using ICP-OES.

Size and chemical composition of wear particles were analyzed by Low Angle Laser Light Scattering (LALLS, Microtrac X100, BioEngineering Solutions Inc) and Scanning Electron Microscope/Energy Dispersive X-ray Spectroscopy (SEM/EDS, JEOL JSM-6490LV).

2.4. Statistics and mathematical response surface

The influence of the three input parameters load, motion amplitude, and applied voltage on total mass loss and wear volume was statistically evaluated using three-way ANOVA (Design Expert Software® version 9, Stat-Ease, Inc., Minneapolis, MN, USA). The response data for both output variables were log-transformed for variance stabilization. The Design Expert software was also used to visualize the corresponding solution space as a response surface. Regression modeling was used to investigate possible associations between primary and secondary outcome variables.

3. Results and analysis

3.1. Measured data from the CoCrMo-discs

Among the different test conditions, given by the combination of the parameters described in Table 1, the total mass loss of the CoCrMo-disc ranged from 0.115 mg to 1.64 mg, and the wear scar volume ranged from 0.0045 mm^3 to 0.0255 mm^3 (average values). No relationship between total mass loss and wear scar volume was found (R^2 = 0.02; Fig. 2A). In order to compare the mass loss with the wear scar volume results, the wear scar volumes were converted into weights using the specific weight of CoCrMo (ρ = 8.3 g/cm^3). This comparison shows, that the total mass loss values were, in all cases, higher than the mass loss values associated with the wear scar itself. Interestingly, the total mass loss of the CoCrMo-disc, tested at open circuit potential with maximal load and maximal motion amplitude (1st additional test), was 0.2 mg, which corresponds well to the value 'y = 0.19' obtained from

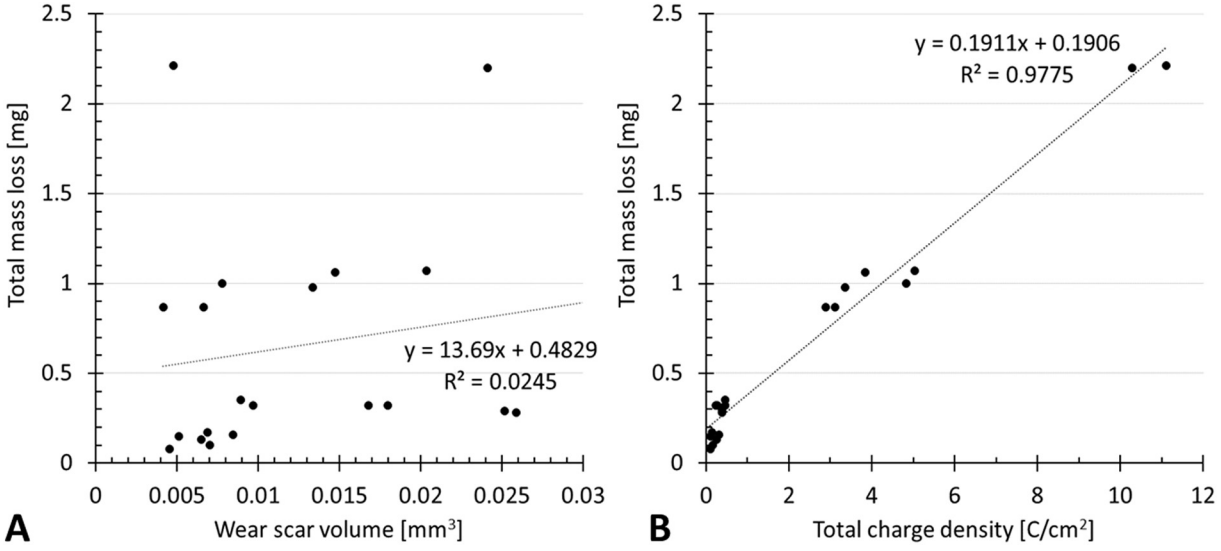

Fig. 2. A) Correlation between wear scar volume and total mass loss from the CoCrMo-discs; B) Correlation between total mass loss of the CoCrMo-discs and total charge density, calculated by integration of the current response to the applied potential during the wear test.

the regression equation in Fig. 2B with 'x = 0' ('y' is the total mass loss and 'x' is the total charge density in Fig. 2B).

The 1st additional test, at maximum load and amplitude at open circuit potential, resulted in 0.0165 mm^3 of wear scar volume, which corresponds to 0.136 mg mass loss, and in a total mass loss of 0.2 mg. The 2nd additional test, run at maximum applied voltage and motion amplitude but without load, resulted in 0.77 mg total mass loss.

3.2. Measured data from media samples

The concentration of Al was below the detection limit (< 0.3 mg/Kg) for all samples, suggesting that the wear of the ceramic ball was negligible. Metal concentrations (Co, Cr and Mo ions and particles) of all media samples and are given in Table 2. The content in medium correlated strongly (R^2 = 0.96), with a regression slope close to 1, to the mass loss of the CoCrMo samples (Fig. 3), suggesting that under all testing conditions, lost material is dispersed in medium. The negative offset in Fig. 3 suggests, that the CoCrMo samples undergo some consistent weight gain, which is bigger at higher potentials. This is in agreement with the formation of deposits observed at the discs tested at +0.9 V. SEM/EDS analysis (not shown) suggested that these deposits are of organic nature. Not surprisingly, a similar strong correlation was found with total charge density. The Co, Cr and Mo content in the medium reflected the composition of the bulk material, considering the Cr/Co and Mo/Co ratios (Table 3), particularly for the tests at +0.9 V applied potential.

The additional test at maximum load and amplitude at open circuit potential had lubricant concentrations of 5.0 mg/kg Co; 1.5 mg/kg Cr; and 0.52 mg/kg Mo.

Table 2
Results from ICP-MS measurements for Co, Cr and Mo concentrations (expressed as mg per kg medium), and respective Cr/Co- and Mo/Co-ratios (right side). The test ID is given by the combination of the three variables: potential (P1 = 0 V; P2 = +0.9 V; P0.5 = +0.45 V); load (L1 = 15 N; L2 = 37 N; L0.5 = 26 N); and amplitude (A1 = 20°; A2 = 40°: A0.5 = 30°).

Test ID	Co [mg/kg]	Cr [mg/kg]	Mo [mg/kg]	Cr/Co [−]	Mo/Co [−]
P1-L1-A1	2	0.47	0.44	0.24	0.22
"	1.5	0.52	0.14	0.35	0.09
P1-L2-A1	1.8	0.68	0.25	0.38	0.14
"	2.2	0.69	0.22	0.31	0.10
P1-L1-A2	4.8	1.5	0.42	0.31	0.09
"	4.9	1.7	0.38	0.35	0.08
P1-L2-A2	6.6	2.4	0.57	0.36	0.09
"	6.7	2.4	0.64	0.36	0.10
P2-L1-A1	62	25	4.4	0.40	0.07
"	15	6.1	1.6	0.41	0.11
P2-L2-A1	13	4.9	1.5	0.38	0.12
"	23	9	1.9	0.39	0.08
P2-L1-A2	19	8.1	1.9	0.43	0.10
"	16	6.4	1.7	0.40	0.11
P2-L2-A2	58	24	4.9	0.41	0.08
"	26	11	2.3	0.42	0.09
P0.5-L0.5-A0.5	2.1	0.63	0.25	0.30	0.12
"	2.7	0.82	0.30	0.30	0.11
"	3.4	0.88	0.29	0.26	0.09
"	4.0	0.99	0.28	0.25	0.07

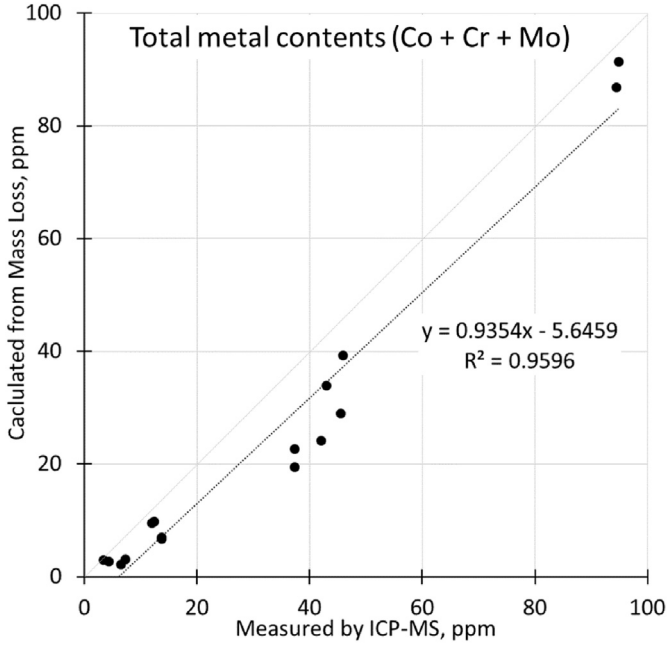

Fig. 3. Correlation between the total metal contents (Co + Cr + Mo), measured by ICP-MS in lubricant samples retrieved after each test, and calculated from the total mass loss values of the CoCrMo samples.

Table 3
Average and standard deviation values of the ratios Cr/Co and Mo/Co for the tests at same applied potential, compared to same ratios for the bulk alloy.

	Cr/Co [−]	Mo/Co [−]
Tests at 0 V (**P1**-…)	0.33 ± 0.05	0.11 ± 0.05
Tests at +0.9 V (**P2**-…)	0.41 ± 0.02	0.09 ± 0.02
Tests at +0.45 V (**P0.5**-…)	0.28 ± 0.03	0.10 ± 0.02
Bulk alloy	0.42	0.09

3.3. Mathematical response surface

The applied potential was the parameter with highest positive impact on the mass loss ($p < .0001$), while it had a weak negative effect on the wear scar volume ($p = .202$). The motion amplitude showed a moderate positive effect on the mass loss ($p = .079$), and a significant positive effect on the wear scar volume ($p < .0001$). The applied load had no statistically significant effect on the mass loss ($p = .949$), while it had a significant positive effect on the wear scar volume ($p < .0001$). Response surfaces were generated for the two most dominating parameters on mass loss (Fig. 4A) and wear scar volume (Fig. 4B). For both responses, the center point data indicated statistically significant ($p \leq .006$) curvature, the center point values lying 41% and 16%, respectively, below the values predicted by their corresponding response surface.

3.4. Wear particles analysis

The metal contents measured by ICP-MS (Table 2) included ions and particles. Since no particles could be detected either by LALLS or by SEM from the tests belonging to the DOE (Table 1), a test with longer duration was run (additional test nr. 3). The results from LALLS were, in terms of mean diameter [μm]: volume (mv) = 7.283; number (mn) = 1.562; area distribution (ma) = 3.811; calculated surface (cs) = 1.575, with standard deviation (sd) = 0.802. According to SEM/EDS analysis from a dried drop of bidistilled water (used to wash the chamber in ultrasonic bath) on a carbon-adhesive stick to the SEM holder, different particles shape and size corresponded different chemical compositions: needle-shaped particles in the size range (1–5) μm contained mostly O, C, P, and Co, with frequent presence of Mg, but absence of Cr; polygonal-shaped particles in the size range (5–10) μm contained mostly O, C, P, Cr, and Co (Fig. 5).

4. Discussion

The bio-tribometer presented in this work allows for the control of the amount of metal released into cell culture medium based on load, amplitude, and applied potential. As next step, we will use the set-up to challenge cells with tribocorrosion degradation products; any electrochemical potential applied between the working electrode (CoCrMo disc) and counter electrode (platinum wire) is expected not to influence the cells response. In fact, the chamber was specially designed, so that the current lines between working and counter electrode are distributed at its upper part, while cell culture dishes are placed at its bottom. In this study, after 12 h of testing, the release of Co fell in the range of 6 to 60 mg/kg (or ppm), which has been reported to decrease cell viability by 30% to 70% [24]. Consequently, we expect that sufficient metal debris can be generated to trigger an immune cell response. Provided that current conditions of the tests after the initial transient current response upon voltage application are stationary, the results from the calibration response surfaces can be extrapolated to test durations longer than the 12 h, up to 48 h, which we take as the upper time limit for the cell culture conditions before the medium needs to be replaced.

The tribocorrosion apparatus allows variation of the ratio of corroded (mostly ions or ion-derived species) to worn (mostly debris) metal released into medium, as indicated by the wide range in the corroded-to-worn metal ratio that was achieved: from 1.3 (input parameters: 40°, 37 N, 0 V) to 41 (20°, 15 N, +0.9 V). In particular, the results from the total mass loss did not correlate with the results from the wear scar volume. The significant effect of the applied potential on the total mass loss, and its insignificant effect on the wear scar volumes indicate that, at the highest potential of +0.9 V (*vs.* SSC), metal dissolution occurred predominantly outside the wear scar. This metal dissolution process was assumed to occur uniformly through the oxide film yielding ionic debris (no macroscopic evidence of any type of corrosion was seen). On the other hand, motion amplitude and load are the parameters that significantly affected wear scar volume. This possibility of varying wear particles *versus* ions needs to be further explored in future studies, for example, by reducing the area of exposed metal not being in contact with the ball, or by starting the test with a more (ball) conforming disc surface.

In anticipation of the next phase of the project, which will include cell culture dishes in the chamber, cell culture medium was chosen as lubricant for this study. This idea is supported by the recent work of Impergre et al. [25], in which cell culture medium was proposed as test fluid for corrosion tests of metallic materials for biomedical

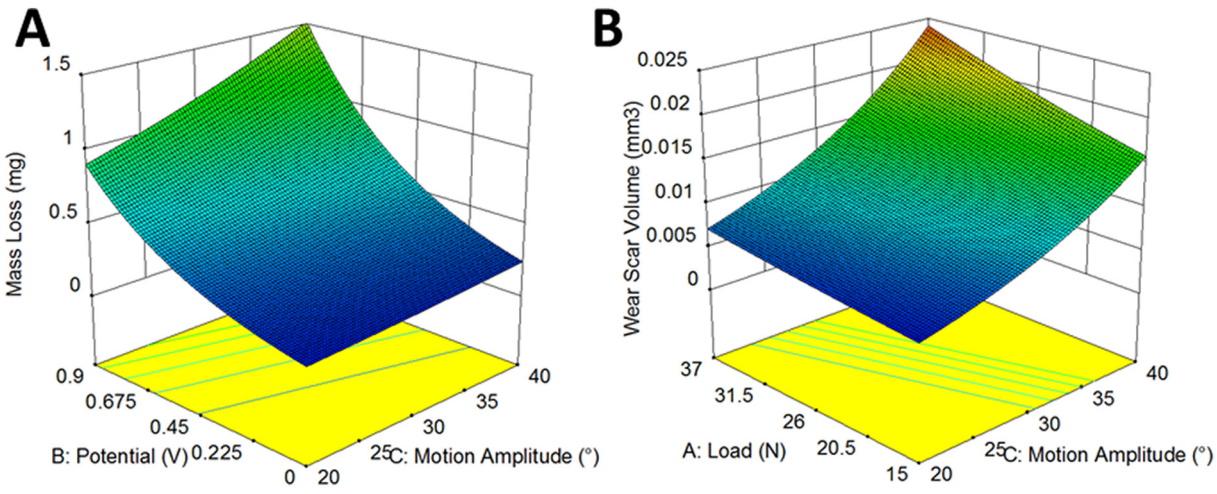

Fig. 4. A) Response surface for the total mass loss as a function of potential and motion amplitude, shown for an intermediate load of 26 N: the potential was the dominant factor affecting the total mass loss, while the dependence on load was weak; B) Calibration response surface for wear scar volume as a function of load and motion amplitude, shown for applied potential 0 V (*vs.* SSC). Load and the motion amplitude were the dominant factors affecting the wear scar volume, while the dependence on potential was weak.

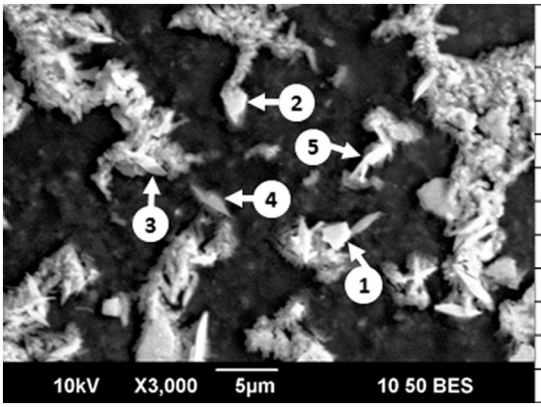

Element	Weight%				
	# 1	# 2	# 3	# 4	# 5
C K	27.35	36.24	25.08	50.07	28.65
O K	33.93	25.38	32.82	29.49	35.74
Na K	1.08	0.66	4.58	-	3.51
P K	3.26	2.87	4.90	4.11	6.99
K K	-	0.70	4.76	-	0.88
Cl K	1.95	-	10.90	-	5.34
Ca K	1.05	0.86	-	-	-
Mg K	-	-	-	0.66	1.18
Cr L	18.51	23.55	-	-	-
Co L	12.87	9.74	16.95	15.68	17.71

Fig. 5. SEM micrograph in backscattered mode (BES) of a dried drop of lubricant, diluted in bidistilled water, from the long test (1,269,000 cycles, 37 N load, 40° amplitude, 0 V *vs.* SSC). Denatured proteinaceous material can be seen around the particles. Results from EDS spectra (10 kV) on different spots are indicated.

applications. In [25], the influence of ambient oxygen, nitrogen, and carbon dioxide on the specific intrinsic electrochemical reactivity of RPMI-1640 was presented. This information is useful for any future study involving potentiostatic or potendiodynamic conditions during wear tests and will help in the interpretation of the current response.

This study is not without limitations. First, regarding the characterization of wear particles produced in the tests belonging to the DOE (12 h), we were limited by a current lack in the technology required for particles digestion and isolation, which are the first steps in a particle characterization protocol for protein containing solutions [26]. Our efforts to find wear particles in the 12 h tests using LALLS and SEM failed. We concluded, that the amount of wear particles generated within the 12 h of the DOE tests was not enough to be detected by LALLS/SEM. We therefore performed the long test (180 h) in order to partially overcome this issue, assuming that the nature of the particles generated by our bio-tribometer would not substantially change with the number of cycles. The results from particles characterization are comparable to corrosion particles found in tissues from patients with total hip replacement [2,27], rather than to wear particles produced either *in-vitro* or *in-vivo* [28,29]; in [2,27], Cr- and Co-phosphate particles in the size range from submicrometer to aggregates as large as 500 μm are documented as corrosion products found in tissues surrounding modular implant junctions. On the other hand, particles generated from CoCrMo-alloy under sliding wear conditions, either in a tribometer or in a hip simulator, were shown to be of smaller size range, from 15 up to 500 nm, with most of the larger particles only partially oxidized with Co only locally and smallest particles made of Cr_2O_3 with no trace of Co [28]. In [29], wear particles isolated from periprosthetic tissues of patients with metal-on-metal hip implants were predominantly nanometer-sized, oval shaped and composed of Cr and O, therefore most probably Cr oxides. We plan to address the characterization of the particles generated in our bio-tribometer in future work, following a published protocol [26]. Second, the reasons for lack of reproducibility in the current response to the applied potential of +0.9 V (*vs.* SSC) must be clarified for future tests. Third, the statistically significant curvature in the response surface indicated by the center point deviation suggests that a more accurate model could be achieved with a quadratic experimental design, such as a central composite [21]. However, the current model is deemed accurate enough for the desired application. Fourth, the experimental protocol has yet to be optimized for cell introduction. Two issues are worth mentioning in this regard. The first is related to the required sterile conditions in the presence of cells. Currently, 3 to 4 min are necessary for test adjustment. During this time, the door of the incubator is open, and this may turn out to be critical for the cell cultures in terms of contamination, pH and/or temperature stability. However, preliminary experiments with cells have been conducted with some success, and we are convinced that this issue can be resolved satisfactorily. The second issue is the application of a potential, required to generate enough tribocorrosion products in the limited time frame of the test, to trigger a measurable immune cell response. Local effects of the applied potential, in particular in the case of +0.9 V, include changes in the pH and oxidation of water. It is unclear, to what extent these local effects will impact the whole system and affect the response of the cells, placed at the bottom of the chamber.

5. Conclusions

- The newly developed bio-tribometer was successfully operated inside a CO_2 incubator. It was able to produce wear and corrosion products from a CoCrMo implant alloy, with the possibility of controlling the ratio of worn to corroded metal by varying the applied potential and the motion amplitude.
- The generated debris recalled corrosion products found in retrieved implants and tissues for size and chemical composition; this aspect yields clinical significance to our study and needs to be further investigated.
- The total concentration of released Co (considered here for its well-known toxicity) corresponded well with the known range to trigger cell response; consequently, we expect our test rig to produce enough metal debris to trigger an immune cell response.
- This bio-tribometer will permit studies on the effect of freshly released metal wear and corrosion products on cells, such as macrophages, lymphocytes, and osteoclasts, or human tissue such as synovium. This approach, which is meant to represent the clinical environment, could provide an opportunity to test cell/tissue tolerance to different materials or could even help to elicit new targets for the improvement of medical implants.

Acknowledgements

The authors thank Stephanie McCarthy, Spencer Fullam, Kyron McAllister (all Rush University Medical Center) and Joel F. Rodriguez, Thomas A. Bruzan, Matthew J. Schuck (UIC scientific instrument shop) for their technical assistance; and Dr. Joachim Kunze for help with the ICP-MS/OES analysis. The authors are particularly thankful for the hospitality and advice provided by Prof. Mathew T. Mathew (University of Illinois, College of Medicine at Rockford).

Funding

This study was supported by the National Institutes of Health (NIH/NIBIB grant number R21EB024039).

Disclosures

The authors have no conflicts of interest to declare.

References

[1] Y. Liao, E. Hoffman, M. Wimmer, A. Fischer, J. Jacobs, L. Marks, CoCrMo metal-on-metal hip replacements, Phys. Chem. Chem. Phy. PCCP 15 (3) (2013), https://doi.org/10.1039/c1032cp42968c.

[2] J.J. Jacobs, J.L. Gilbert, R.M. Urban, Current concepts review – corrosion of metal orthopaedic implants, J. Bone Joint Surg. Am. 80 (2) (1998) 268–282.

[3] H.J. Cooper, R.M. Urban, R.L. Wixson, R.M. Meneghini, J.J. Jacobs, Adverse local tissue reaction arising from corrosion at the femoral neck-body junction in a dual-taper stem with a cobalt-chromium modular neck, J. Bone Joint Surg. Am. 95 (10) (2013) 865–872, https://doi.org/10.2106/JBJS.L.01042.

[4] I.P. Gill, J. Webb, K. Sloan, R.J. Beaver, Corrosion at the neck-stem junction as a cause of metal ion release and pseudotumour formation, J. Bone Joint Surg. Br 94 (7) (2012) 895–900, https://doi.org/10.1302/0301-620X.94B7.29122.

[5] D.R. Plummer, R.A. Berger, W.G. Paprosky, S.M. Sporer, J.J. Jacobs, C.J. Della Valle, Diagnosis and management of adverse local tissue reactions secondary to corrosion at the head-neck junction in patients with metal on polyethylene bearings, J. Arthroplast. 31 (1) (2016) 2684–2688, https://doi.org/10.1016/j.arth.2015.07.039.

[6] B.J. McGrory, J. MacKenzie, G. Babikian, A high prevalence of corrosion at the head-neck taper with contemporary Zimmer non-cemented femoral hip components, J. Arthroplast. 30 (7) (2015) 1265–1268, https://doi.org/10.1016/j.arth.2015.02.019.

[7] I. Catelas, M.A. Wimmer, S. Utzschneider, Polyethylene and metal wear particles: characteristics and biological effects, Semin. Immunopathol. 33 (3) (2011) 257–271, https://doi.org/10.1007/s00281-011-0242-3.

[8] K. Merritt, S.A. Brown, Release of hexavalent chromium from corrosion of stainless steel and cobalt-chromium alloys, J. Biomed. Mater. Res. 29 (5) (1995) 627–633.

[9] E.J. Martin, R. Pourzal, M.T. Mathew, K.R. Shull, Dominant role of molybdenum in the electrochemical deposition of biological macromolecules on metallic surfaces, Langmuir 29 (15) (2013) 4813–4822, https://doi.org/10.1021/la304046q.

[10] I. Milošev, M. Remškar, In vivo production of nanosized metal wear debris formed by tribochemical reaction as confirmed by high-resolution TEM and XPS analyses, J. Biomed. Mater. Res. A 91A (4) (2009) 1100–1110, https://doi.org/10.1002/jbm.a.32301.

[11] Y. Liao, R. Pourzal, M.A. Wimmer, J.J. Jacobs, A. Fischer, L.D. Marks, Graphitic tribological layers in metal-on-metal hip replacements, Science 334 (6063) (2011) 1687–1690, https://doi.org/10.1126/science.1213902.

[12] R. Pourzal, R. Theissmann, S. Williams, B. Gleising, J. Fisher, A. Fischer, Subsurface changes of a MoM hip implant below different contact zones, J. Mech. Behav. Biomed. Mater. 2 (2) (2009) 186–191, https://doi.org/10.1016/j.jmbbm.2008.08.002.

[13] M. Lyvers, D.R. Bijukumar, A. Moore, P. Saborio, D. Royhman, M.A. Wimmer, K. Shull, M.T. Mathew, Electrochemically generated tribolayer on CoCrMo metal for hip implant applications: in vitro evaluation of stability (Tribocorrosion kinetics) and biocompatibility, Paper Presented at the ORS 2017 Annual Meeting, 2017.

[14] H. Zhou, K. Zhao, W. Li, N. Yang, Y. Liu, C. Chen, T. Wei, The interactions between pristine graphene and macrophages and the production of cytokines/chemokines via TLR- and NF-kappaB-related signaling pathways, Biomaterials 33 (29) (2012) 6933–6942, https://doi.org/10.1016/j.biomaterials.2012.06.064.

[15] K. Merritt, L. Wenz, S.A. Brown, Cell association of fretting corrosion products generated in a cell culture, J. Orthop. Res. 9 (2) (1991) 289–296, https://doi.org/10.1002/jor.1100090218.

[16] R. Pourzal, R. Cichon, M.T. Mathew, C.A. Pacione, A. Fischer, N. Hallab, M.A. Wimmer, Design of a tribocorrosion bioreactor for the analysis of immune cell response to in situ generated wear products, J. Long-Term Eff. Med. Implants 24 (1) (2014) 65–76.

[17] A. Fischer, D. Janssen, M.A. Wimmer, The influence of molybdenum on the fretting corrosion behavior of CoCr/TiAlV couples, 11 (2017), https://doi.org/10.1016/j.biotri.2017.01.001.

[18] A.J. Bard, L.R. Faulkner, Electrochemical Methods: Fundamentals and Applications, Wiley, 2000.

[19] S. Mischler, A. Igual Munoz, Wear of CoCrMo alloys used in metal-on-metal hip joints: a tribocorrosion appraisal, Wear 297 (2013) 1081–1094.

[20] G.E.P. Box, N.R. Draper, Response Surfaces, Mixtures, and Ridge Analyses, Probability and Statistics, 2, John Wiley & Sons, Inc, Hoboken, NJ, USA, 2007, , https://doi.org/10.1002/0470072768.

[21] M.A. Bezerra, R.E. Santelli, E.P. Oliveira, L.S. Villar, L.A. Escaleira, Response surface methodology (RSM) as a tool for optimization in analytical chemistry, Talanta 76 (5) (2008) 965–977, https://doi.org/10.1016/j.talanta.2008.05.019.

[22] M.T. Mathew, T. Uth, N.J. Hallab, R. Pourzal, A. Fischer, M.A. Wimmer, Construction of a tribocorrosion test apparatus for the hip joint: validation, test methodology and analysis, Wear 271 (9–10) (2011) 2651–2659, https://doi.org/10.1016/j.wear.2011.01.085.

[23] M.A. Wimmer, M.P. Laurent, M.T. Mathew, C. Nagelli, Y. Liao, L.D. Marks, J.J. Jacobs, A. Fischer, The effect of contact load on CoCrMo wear and the formation and retention of tribofilms, Wear 332 (333) (2015) 643–649, https://doi.org/10.1016/j.wear.2015.02.013.

[24] Y.-M. Kwon, Z. Xia, S. Glyn-Jones, D. Beard, H.S. Gill, D.W. Murray, Dose-dependent cytotoxicity of clinically relevant cobalt nanoparticles and ions on macrophages in vitro, Biomed. Mater 4 (2) (2009) 025018.

[25] A. Impergre, B. Ter-Ovanessian, C. Der Loughian, B. Normand, Systemic strategy for biocompatibility assessments of metallic biomaterials: representativeness of cell culture medium, Electrochim. Acta 283 (2018) 1017–1027, https://doi.org/10.1016/j.electacta.2018.06.196.

[26] F. Billi, P. Benya, A. Kavanaugh, J. Adams, H. McKellop, E. Ebramzadeh, The John Charnley award: an accurate and extremely sensitive method to separate, display, and characterize wear debris: part 2: metal and ceramic particles, Clin. Orthop. Relat. Res. 470 (2) (2012), https://doi.org/10.1007/s11999-011-2058-9.

[27] D. Hall, R. Pourzal, C.J. Della Valle, J.O. Galante, J.J. Jacobs, R.M. Urban, Corrosion of modular junctions in femoral and acetabular components for hip arthroplasty and its local and systemic effects, Modularity and Tapers in Total Joint Replacement Devices, ASTM International, 2015, pp. 410–427, , https://doi.org/10.1520/stp159120140134 vol STP 1951.

[28] R. Pourzal, I. Catelas, R. Theissmann, C. Kaddick, A. Fischer, Characterization of wear particles generated from CoCrMo alloy under sliding wear conditions, Wear 271 (9–10) (2011) 1658–1666, https://doi.org/10.1016/j.wear.2010.12.045.

[29] I. Catelas, P.A. Campbell, J.D. Bobyn, J.B. Medley, O.L. Huk, Wear particles from metal-on-metal total hip replacements: effects of implant design and implantation time, Proc. Inst. Mech. Eng. H 220 (2) (2006) 195–208, https://doi.org/10.1243/09544119JEIM112 2006 Feb.